



Schmidt Hammer exposure dating (SHED)

DOI:

[10.1016/j.quageo.2017.12.003](https://doi.org/10.1016/j.quageo.2017.12.003)

Document Version

Accepted author manuscript

[Link to publication record in Manchester Research Explorer](#)

Citation for published version (APA):

Tomkins, M. D., Huck, J., Dortch, J. M., Hughes, P. D., Kirbride, M. P., & Barr, I. D. (2018). Schmidt Hammer exposure dating (SHED): Calibration procedures, new exposure age data and an online calculator. *Quaternary Geochronology*, 44, 55-62. <https://doi.org/10.1016/j.quageo.2017.12.003>

Published in:

Quaternary Geochronology

Citing this paper

Please note that where the full-text provided on Manchester Research Explorer is the Author Accepted Manuscript or Proof version this may differ from the final Published version. If citing, it is advised that you check and use the publisher's definitive version.

General rights

Copyright and moral rights for the publications made accessible in the Research Explorer are retained by the authors and/or other copyright owners and it is a condition of accessing publications that users recognise and abide by the legal requirements associated with these rights.

Takedown policy

If you believe that this document breaches copyright please refer to the University of Manchester's Takedown Procedures [<http://man.ac.uk/04Y6Bo>] or contact uml.scholarlycommunications@manchester.ac.uk providing relevant details, so we can investigate your claim.



Schmidt Hammer exposure dating (SHED): Calibration procedures, new exposure age data and an online calculator

Tomkins, M.D., Huck, J.J., Dortch, J.D., Hughes, P.D., Kirkbride, M.P., and Barr, I.D.

Abstract

Recent research has established Schmidt Hammer exposure dating (SHED) as an effective method for dating glacial landforms in the UK. This paper presents new data and discussion to clarify and to evaluate calibration procedures. These make a distinction between Schmidt Hammer drift following use (*instrument calibration*), and variation between both individual Schmidt Hammers and between user strategies when utilising age-calibration curves (*age calibration*). We show that while test anvil methods are useful for verifying that Schmidt Hammers maintain their standard R-values, they are inappropriate for instrument calibration except for the hardest natural rock surfaces (R-values: ≥ 70). A range of surfaces were tested using 3 N-Type Schmidt Hammers, which showed that existing anvil calibration procedures led to consistent overestimation of R-values by up to 17.9%. In contrast, new calibration procedures, which are based on the use of a calibration point which lies within the range of R-values measured in the field [Dortch *et al.* 2016, *Quat. Geochron.*, 35, 67-68], limit variance to maximum of 4.4% for surfaces typically tested by Quaternary researchers (R-values: 25 - 60). Moreover, these new calibration procedures are more appropriate for age calibration as they incorporate operator variance through choice of sampling location. New calibration procedures are used to compile an updated age-calibration curve based upon 54 granite surfaces ($R^2 = 0.94$, $p < 0.01$) from across Scotland, NW England and Ireland. The inclusion of a further 29 terrestrial cosmogenic nuclide (TCN) exposure ages extends the calibration period to 0.8 – 23.8 ka, covering the entire post-Last Glacial Maximum (LGM) history of the British-Irish Ice Sheet. To facilitate comparison between studies, an online calculator is made available at <http://shed.earth> for Schmidt Hammer instrument and age calibration and SHED exposure age calculation. The SHED-Earth calculator provides a rapid and accessible means of exposure age calculation to encourage wider and more consistent application of SHED throughout the British Isles.

Introduction

In a recent study by Tomkins *et al.* (2016), a statistically significant relationship ($R^2 = 0.81$, $p < 0.01$) was observed between the terrestrial cosmogenic nuclide (TCN) exposure ages and Schmidt Hammer rebound values (R-values) of 25 granitic surfaces from Scotland and NW England (Phillips *et al.*, 2008; Small *et al.*, 2012; Wilson *et al.*, 2013; Kirkbride *et al.*, 2014). These data indicate that granite can weather linearly over significant spatial scales for regions of similar climate (Tomkins *et al.*, 2016). The associated calibration curve was applied to undated glacial erratics ($n = 31$) on Shap Fell, NW England and generated a deglacial age of 16.5 ± 0.5 ka, a result which corroborates with existing methods (Wilson *et al.*, 2013) and is of comparable accuracy and precision to proximal TCN exposure ages. Using the University of Manchester calibration boulder (Dortch *et al.*, 2016), a recent study in the Mourne Mountains, Northern Ireland (Barr *et al.*, 2017), applied the Tomkins *et al.* (2016) SHED calibration curve to undated granite surfaces and generated a deglacial chronology that was consistent with existing interpretations of post-Last Glacial Maximum (LGM) glaciation in that region (Wilson, 2004; McCabe *et al.*, 2007; McCabe and Williams, 2012). As there were previously

43 no published numerical ages to constrain the chronology of glaciation (Barr *et al.*, 2017), these new
44 data provide an important geochronological control on Lateglacial and Younger Dryas ice dynamics
45 in the Mourne. While SHED age estimates were generally younger (more recent) than established
46 chronologies, perhaps reflecting climatic or lithological variation, the SHED approach was able to
47 differentiate clearly between different phases of glaciation and is considered a viable method for
48 constraining the extent of this region's glaciers during the Younger Dryas (Barr *et al.*, 2017).

49 However, Winkler and Matthews (2016) contend that the real potential of SHED has been
50 undermined by inappropriate calibration procedures utilised in Tomkins *et al.*, (2016) and presented
51 in Dortch *et al.*, (2016). Here, we present new data and discussion to evaluate this issue in a robust
52 and quantitative way. To assess the effectiveness of these calibration procedures and by association,
53 the suitability of our regional calibration curve (Tomkins *et al.*, 2016), we have compiled an updated
54 calibration curve with new exposure age data from the Holocene (Kirkbride *et al.*, 2014), Younger
55 Dryas (Small and Fabel, 2016) and Lateglacial Interstadial (Everest and Kubik, 2006; Finlayson *et al.*,
56 2014). In addition, we include early post-LGM (18 – 24 ka) exposure ages from Wexford (Ballantyne
57 and Stone, 2015) and Donegal, Ireland (Ballantyne *et al.*, 2007; Clark *et al.*, 2009). These new data (n
58 = 29) extend the calibration period to 0.8 – 23.8 ka, covering the entire post-Last Glacial Maximum
59 (LGM) history of the British-Irish Ice Sheet (Clark *et al.*, 2012).

60 While this regional calibration curve is unlikely to be globally applicable, as long-term weathering
61 rates exhibit systematic variability between diverse climatic regimes (Riebe *et al.*, 2004; von
62 Blanckenburg *et al.*, 2015), our methods can be used to develop similarly robust SHED calibration
63 curves in other well-dated regions. This study aims to enable this by:

- 64 1. Testing and clarifying Schmidt Hammer calibration procedures. We make a distinction
65 between *instrument calibration* i.e. correcting for Schmidt Hammer drift following use, and *age*
66 *calibration* i.e. correcting different Schmidt Hammers and user strategies to a verifiable
67 standard prior to the utilisation of our regional calibration curve.
- 68 2. Presenting new evidence to update and reinforce our regional SHED calibration curve.
- 69 3. Providing an online calculator for Schmidt Hammer instrument and age calibration and SHED
70 exposure age calculation at <http://shed.earth> to encourage wider and more consistent
71 application of SHED throughout the British Isles.

72

73 **Instrument calibration**

74 In their comment on Dortch *et al.* (2016), Winkler and Matthews (2016) criticise our calibration
75 procedures as being unnecessary, impractical and less accurate than existing methods (Proceq, 2004;
76 Aydin, 2009). In addition, the authors argue that our term 'standardised R-values' creates confusion
77 as it does not differentiate clearly between instrument calibration and converting R-values into age
78 information when developing a SHED-calibration curve.

79 Existing ISRM calibration procedures recommend the use of the test anvil to account for R-value
80 drift following intensive use (Aydin, 2009). The test anvil should yield R-values in the range of 81 ± 2
81 for N-type Schmidt Hammers which have specified impact energies of 2.207 Nm (Proceq, 2004).
82 Schmidt Hammers should be calibrated before and after use to generate a correction factor (CF)
83 which should be applied to all readings as follows:

$$CF = \frac{\text{Specified standard value of the anvil}}{\text{Average of ten readings on the anvil}}$$

84 Test anvils are constructed with vertically guided impact points made of steel as hard as that of the
 85 plunger tip (Aydin, 2009) and thus amplify variation between pre- and post-use calibration values and
 86 variation between different Schmidt Hammers (McCarroll, 1987). An implicit assumption in this
 87 calibration procedure is that the difference (%) between the specified anvil standard and the average
 88 of 10 readings is consistent throughout the operational range of the Schmidt Hammer (Compressive
 89 strength 10 - 70 N/mm²; Proceq, 2004). However, very few natural rock surfaces generate R-values
 90 at the upper end of this operational range (c.f. Table 1 in Goudie, 2006; 17/110 entries record R-
 91 values ≥ 60 , 1/110 entries record R-values ≥ 70). As such, it is clearly necessary to evaluate the
 92 effectiveness of the standard calibration procedures (Proceq, 2004; Aydin, 2009) on surfaces of
 93 varying hardness to establish their validity (Winkler and Matthews, 2016).

94 To test this, we sampled a range of surfaces using three N-type Schmidt Hammers of varying age and
 95 usage (New Proceq: NPC, New NovaTest: NT, Old Proceq: OPC), all with specified impact energies
 96 of 2.207 Nm. 30 R-values were generated for each surface by the same operator and followed the
 97 procedures outlined by Viles *et al.* (2011). The sampling strategy was consistent for each test, while
 98 each surface was sampled on the same day to minimise the effect of variability in rock (Sumner and
 99 Nel, 2002) or surface moisture content (Viles *et al.*, 2011). Carborundum pre-treatment was
 100 performed for each surface to minimise potential errors resulting from variable surface roughness.
 101 Sample information and results are presented in Table 1.

102 The mean test anvil R-values varied significantly (NPC = 84 ± 0 , NT = 79.3 ± 0.7 , OPC = 67.5 ± 2.6),
 103 reflecting the varying usage of each Schmidt Hammer. However, these data demonstrate that the
 104 difference (%) between the Schmidt Hammers as recorded using the test anvil (NT = 5.6%, OPC =
 105 19.6%) is not maintained throughout the operational range of the Schmidt Hammer (Fig. 1). Instead,
 106 the difference (%) between each tool decreases significantly as the surface R-value decreases. Of
 107 particular note is the consistency of mean R-values for the NPC and NT for the 3 weakest surfaces
 108 (R-values ≤ 48). The variance between the NPC and NT for these surfaces is not statistically
 109 significant as determined by Students T-tests (Table 1). The calibration procedures of Aydin (2009)
 110 were applied to the NT and OPC, with correction factors of 1.059 and 1.244 respectively, and
 111 compared to the values generated by the NPC (Table 2). To provide a baseline of measurement, we
 112 explicitly assume that the values generated by the NPC are a 'true' measure of the rock surface R-
 113 value. However, we acknowledge that a 'true' surface R-value is indeterminable (McCarroll, 1987) as
 114 this would require validation through repeated Schmidt Hammer testing which in turn could be
 115 affected by R-value drift following use, operator variance or even variance between new Schmidt
 116 Hammers (McCarroll, 1987). Ideally, we would have tested each Schmidt Hammer on surfaces with
 117 specified R-values but with the exception of the test anvil, these are not available. However, the
 118 NPC generated consistent values on the test anvil (84 ± 0) and we use these data as the basis for
 119 our calculations. Existing recalibration procedures result in consistent R-value overestimation in the
 120 typical 25 - 60 R-value operational range (Goudie, 2006), equivalent to 3.4 - 7.2% for the NT (Fig.
 121 2B) and 9.2 - 17.9% for the OPC (Fig. 2A).

122 Next, we evaluate the calibration procedures of Dortch *et al.* (2016) using a calibration surface
 123 within the range of the sample data. Schmidt Hammers were recalibrated using the University of
 124 Manchester calibration boulder (Doddington Sandstone boulder; 1.8 m x 0.7 m x 0.7 m (L x W x H);
 125 NPC R-value 47.4 ± 1.9 ; NT R-value 47.6 ± 2.1 , OPC R-value 43.5 ± 1.8) giving CFs of 0.994 and

126 1.167 for the NT and OPC respectively (Dortch *et al.*, 2016). Recalibrated R-values correspond
127 more closely to baseline NPC values, differing by a maximum of 2.9% for the NT (Fig. 2B) and 4.4%
128 for OPC (Fig. 2A) within the typical 25 - 60 R-value operational range (Table 2). It must be noted
129 that the data diverge towards the upper limit of the tools' operational range, as this calibration
130 underestimates R-values for the two hardest surfaces by 3.4 - 6.1% for the NT and 6.6 - 12.4% for
131 the OPC. However, from a combined total of 295 samples reported by Goudie (2006), Tomkins *et al.*
132 *et al.* (2016), and Barr *et al.* (2017), 277 or 93.9% have mean R-values within the range 25 - 60. For
133 these surfaces, the variation between the NPC and the NT-OPC is reduced to a maximum of just
134 4.4% as compared to 17.9% for the ISRM method.

135 These data demonstrate that R-value data should be recalibrated using a calibration point which is
136 within the range of sample data (Dortch *et al.*, 2016). A boulder of sufficient size (Sumner and Nel,
137 2002; Demirdag *et al.*, 2009), that is free of surface discontinuities (Williams and Robinson, 1983)
138 and lichen (Matthews and Owen, 2008) and is easily accessible would be ideal. The University of
139 Manchester calibration boulder as used in Tomkins *et al.* (2016) and presented in Dortch *et al.*
140 (2016) is ideally suited for instrument calibration, as it is within the range of surfaces typically tested
141 by Quaternary researchers (R-value: 48.08 ± 0.82). For clarity, we are not advocating that
142 researchers must use the University of Manchester calibration boulder for *instrument calibration*,
143 although we do encourage users to perform *age calibration* using this surface in order to test or
144 utilise the regional calibration curve (see below). However, we are advocating that researchers use a
145 *comparable* surface to perform instrument calibration i.e. one that returns R-values within the range
146 of field data, is free of surface discontinuities and is easily accessible. Moreover, researchers should
147 follow our sampling methodology and perform carborundum pre-treatment to ensure a smooth,
148 debris-free surface. Users should record 30 R-values perpendicular to the tested surface to reduce
149 the risk of frictional sliding of the plunger tip (Viles *et al.*, 2011), with single impacts separated by at
150 least a plunger width (Aydin, 2009). As the SH is sensitive to rock (Sumner and Nel, 2002) and
151 surface moisture content (Viles *et al.*, 2011), we recommend sampling in dry conditions. For very
152 hard rock surfaces (R-values: ≥ 70), the test anvil method may be effective as variation between
153 Schmidt Hammers as recorded on the anvil is probably representative of variability on sampled rock
154 surfaces (Table 2). However, while we do not dispute the value of the test anvil in verifying that
155 Schmidt Hammers maintain their standard R-values and for prompting cleaning or repair (Winkler
156 and Matthews, 2016), it is clear that instrument calibration using the test anvil will significantly
157 overestimate R-values for the vast majority of rock surfaces tested by Quaternary researchers (R-
158 values: ≤ 60).

159

160 **Age calibration**

161 In their comment on Dortch *et al.*, (2016), Winkler and Matthews (2016) are correct in their
162 assertion that "Standardisation of R-values is irrelevant for the construction of these calibration
163 curves because their accuracy relies on the quality of those specific control points and a consistent
164 sampling design throughout data collection." However, unlike previous studies, which generate
165 localised age calibration curves (i.e. single valley), the goal of the SHED project was to encourage
166 researchers to test and use our calibration curve on undated landforms at the regional scale and
167 compare results with independent dating methods (e.g. TCN, ^{14}C , OSL) to evaluate its effectiveness
168 as a geochronological tool. Thus, "age calibration" relates to the *utilisation*, not the *construction*, of
169 calibration curves. As a result, the standardisation of different Schmidt Hammers (McCarroll, 1987)

170 and different user strategies (Viles *et al.*, 2011) to a verifiable standard is necessary to limit potential
171 errors in SH exposure age estimates.

172 Age calibration could be undertaken using the test anvil but this is rejected for two reasons. Firstly,
173 as with instrument calibration, the difference between Schmidt Hammers as recorded using the test
174 anvil is unlikely to be replicated on surfaces typically tested by Quaternary researchers and would
175 likely result in significant R-value overestimation. Secondly, the test anvil procedures of McCarroll
176 (1987; 1994) and Aydin (2009), and calibration guidelines from Proceq (2004), consider instrument
177 error but do not account for the uncertainty generated by user variance. Viles *et al.*, (2011) state
178 that “operator variance ... may also be an issue even for well-established techniques such as the
179 Schmidt Hammer”. Variance between users, due to choice of sampling location or operating
180 procedure, cannot be discounted as a source of error in R-value data and subsequent SH exposure
181 age estimates. As a result, the use of a natural rock surface (University of Manchester calibration
182 boulder) is more appropriate for age calibration as it simulates field sampling conditions and permits
183 R-value variation due to (1) choice of sampling location and (2) sampling strategy. While “micro-scale
184 inhomogeneity of the sandstone” will result in larger uncertainties than the test anvil methods
185 (Winkler and Matthews, 2016), we consider this marginal increase in uncertainty to be insufficient to
186 offset the considerable advantages of (1) incorporating operator variance and (2) enabling
187 recalibration without significant overestimation.

188 It is vitally important for the development of SHED, and the trust of the geomorphological
189 community, that unrealistically precise estimates are avoided in the literature. However, while errors
190 in instrument and age calibration could influence SH exposure age estimates, it is clear that the
191 largest uncertainties in SHED are a consequence of limited control points for age-calibration curve
192 construction (Winkler, 2009; Matthews and Winkler, 2011). This is exacerbated by geological
193 uncertainty associated with TCN exposure ages (Heyman *et al.*, 2011) which may adversely affect
194 calibration curves based on sparse and isolated control points (Tomkins *et al.*, 2016). As a result,
195 local ‘R-value to age’ calibration curves with limited age control points are unlikely to be applicable
196 on a wider regional scale. Even robust age calibration curves ($R^2 = 0.94$, $p = < 0.01$), based upon
197 significant exposure age data sets ($n = 54$), must avoid unrealistically precise estimates of surface
198 exposure age if the Quaternary community at large is to take up the Schmidt Hammer and integrate
199 it with radiometric dating methods. To that end, the instrument and age calibration procedures
200 outlined here are suitable for the geomorphological community as they work effectively on surfaces
201 typically tested by Quaternary researchers (R-values: 25 - 60) and minimise potential errors
202 introduced by variation between Schmidt Hammers and between user strategies.

203 As a result, we provide the following recommendations:

- 204 1. *Instrument calibration* - Users can account for R-value drift following use using a suitable
205 surface before and after sampling following the methods presented in Dortch *et al.* (2016).
206
- 207 2. *Age calibration* – Users can account for variation between Schmidt Hammers and between
208 user strategies by calibrating their Schmidt Hammer using the University of Manchester
209 calibration boulder to standardise R-values to our regional calibration curve.
210
- 211 3. *Exposure-age calculation* – Users can input instrument and age calibration values and raw R-
212 value data into the SHED-Earth online calculator (<http://shed.earth>) to generate SH

213 exposure ages and 1σ uncertainties based on the updated calibration curve presented in this
214 study.

215

216 4. *Developing an independent regional age calibration curve* – To generate a new exposure age to
217 R-value calibration curve in a similar well-dated region, first select a suitable surface for age
218 calibration. This surface should be tested before all field-testing to minimise errors due to
219 variation between Schmidt Hammers and between user strategies. The location of this
220 surface should be published to encourage wider use (Dortch *et al.*, 2016). Next, select a
221 suitable surface for instrument calibration. This surface should be used before and after all
222 field-testing to account for R-value drift. Finally, proceed to develop a calibration dataset for
223 your region.

224

225 **Updating the UK SHED calibration curve**

226 These instrument and age calibration procedures are used to compile an updated age-calibration
227 curve based on upon 54 granite surfaces ($R^2 = 0.94$, $p = < 0.01$) from across Scotland, NW England
228 and Ireland. This calibration curve comprises a further 29 TCN exposure age control points (Figs. 3)
229 and includes new Holocene and Younger Dryas exposure ages from moraine crests in Coire an
230 Lochain, Cairngorms (Fig. 4A; $n = 5$, 0.8 – 5.5 ka; Kirkbride *et al.*, 2014) and on Rannoch Moor,
231 Scottish Highlands (Fig. 4B; $n = 5$, 11.2 – 12.7 ka; Small and Fabel, 2016), in addition to Lateglacial
232 exposure ages from Glen Einich, Cairngorms (Fig. 4C; $n = 6$, 14.3 – 16.8 ka; Everest and Kubik,
233 2006) and Glen Iorsa, Arran ($n = 2$, 15.8 – 16.7 ka; Finlayson *et al.*, 2014). Dated surfaces from Glen
234 Einich were not included in the previous calibration curve (Tomkins *et al.*, 2016) due to their coarse-
235 grained surface texture and poor internal ‘exposure age to R-value’ consistency ($R^2 = 0.19$, $p = 0.39$).
236 However, on further analysis, we note that four of the six exposure ages were within 1σ uncertainty
237 of the original calibration regression. In addition, their lack of internal consistency is probably best
238 accounted for by TCN exposure age uncertainty ($\pm 1.1 - 1.6$ ka). For transparency, all of these data
239 are included. Finally, we include early post-LGM exposure ages from Blackstairs Mountain, Wexford
240 ($n = 2$, 23.3 – 23.4 ka; Ballantyne and Stone, 2015) and Bloody Foreland, Donegal (Fig. 4D; $n = 8$,
241 18.2 – 23.8 ka; Ballantyne *et al.*, 2007; Clark *et al.*, 2009). These data fit the trend established at early
242 (> 20 ka) post-LGM sites from Buchan (Phillips *et al.*, 2008) and demonstrate the wide applicability of
243 this calibration curve throughout the British Isles. As a result, the comparatively ‘young’ SHED
244 exposure age estimates from the Mourne Mountains (Barr *et al.*, 2017) appear unlikely to reflect
245 climatic variation.

246 All calibration curve exposure ages were calculated using the online calculators formerly known as
247 the CRONUS-Earth online calculators (<http://hess.ess.washington.edu/math/>, Wrapper script 2.3,
248 Main calculator 2.1, constants 2.3, muons 1.1; Balco *et al.*, 2008). Exposure ages are based on the
249 time-dependent L_m scaling (Lal, 1991; Stone, 2000) and assuming 0 mm ka^{-1} erosion. While there are
250 no reliable estimates of surface erosion rates for rock surfaces in the British Isles (Ballantyne, 2010),
251 erosion rates for most crystalline glaciated rock surfaces are usually low (0.1 – 0.3 mm ka^{-1} ; André,
252 2002). As such, assuming 0 mm ka^{-1} of surface erosion is the most suitable approach as rates of
253 surfaces lowering are likely negligible (André, 2002) and should not be estimated without
254 supplementary data. Exposure ages are based on the Loch Lomond production rate (LLPR; Fabel *et al.*
255 *et al.*, 2012) of 4.02 ± 0.18 atoms $g^{-1} a^{-1}$. The LLPR is based on ^{10}Be concentrations from erratic
256 boulders on the terminal moraine of the Younger Dryas Loch Lomond glacier advance (Fabel *et al.*,
257 2012), the timing of which is independently constrained by ^{14}C ages (MacLeod *et al.*, 2011). The LLPR

258 is the default production rate for the SHED-Earth online calculator although we also include the
259 option to calculate ages based on the Glen Roy production rate (GRPR; Small and Fabel, 2015) and
260 the primary calibration dataset of Borchers et al., (2016) for comparison. The full exposure age
261 calibration dataset is available in Appendix I.

262 In total, this updated calibration curve (Fig. 5) is based on 54 dated surfaces from across Scotland,
263 NW England and Ireland, and definitively demonstrates a clear correlation between exposure ages
264 and recalibrated R-values ($R^2 = 0.94$, $p = < 0.01$). For individual SH exposure age estimates that fall
265 within the operational range of our calibration curve (0.8 – 23.8 ka), this technique generates typical
266 errors of ~1.4 ka, reflecting the uncertainty introduced by (1) recorded scatter in SH R-values and
267 (2) intrinsic uncertainty associated with calibration curve TCN ages. However, in aggregate,
268 internally-consistent SH exposure age datasets (e.g. $n = 30$) can be of comparable precision to TCN
269 ages (Tomkins et al., 2016), as counting statistics can be used to consolidate probability when
270 numerous ages are obtained. The addition of new exposure ages to the calibration curve has
271 changed the slope of the calibration curve regression (Tomkins et al., 2016: $y = -0.4881x + 34.834$,
272 updated curve: $y = -0.5678x + 37.692$). To evaluate the significance of this change, we recalibrated
273 the Shap Fell data presented in Tomkins et al., (2016). Using the original calibration regression, this
274 data generated a mean exposure age of 16.5 ± 0.5 ka and provided a limiting age for the south-
275 westerly retreat of ice towards the mountains of the Lake District (Wilson, 2016). Using the
276 updated calibration regression, the arithmetic mean and mean absolute deviation of this dataset is
277 16.36 ± 0.60 ka ($n = 31$). This estimate is consistent with the youngest LLPR TCN exposure age
278 from Shap Fell of 16.42 ± 0.98 ka (Wilson et al., 2013). As such, the application of the updated
279 calibration curve to these data has no impact on the conclusions of Tomkins et al., (2016).

280

281 **SHED online calculator**

282 A key objective of the SHED project is to make our calibration curve accessible to Quaternary
283 researchers and thus enable wider and more consistent application of the technique to undated
284 landscapes (c.f. Barr et al., 2017). To that end, we present a tool for Schmidt Hammer instrument
285 and age calibration and SHED exposure age calculation (available at <http://shed.earth>). SHED-Earth
286 performs the following functions:

287 1. *Instrument calibration* – Users can input raw R-value data in chronological order (related to
288 the time of sampling, not the SHED chronology) and the R-values of their instrument
289 calibration surface before and after sampling. R-values will be corrected assuming linear R-
290 value drift (Tomkins et al., 2016). This procedure is most effective when periods between
291 calibration tests are short (McCarroll, 1987). While we encourage users to record 30 R-
292 values per surface to ensure statistically significant results, the tool will also operate on
293 variable sample sizes (c.f. Table 2 in Niedzielski et al., 2009).

294

295 2. *Age calibration* – Users can input the mean value recorded for the University of Manchester
296 calibration boulder and the tool will correct each R-value using a correction factor (%).
297 Users who have not completed age calibration using the University of Manchester calibration
298 boulder should use the default value (R-value: 48.08 ± 0.82). This is the mean R-value
299 generated by the Proceq N-type Schmidt Hammer used to generate the original calibration
300 curve (Tomkins et al., 2016). As such, no correction for variation between different Schmidt
301 Hammers or between user strategies will be made. Although variance between Schmidt

Hammers is usually small for surfaces with R-values of ≤ 60 , and should be minimal if Schmidt Hammers are calibrated on a regular basis, variance can exceed ~10% for older Schmidt Hammers (Table 2; OPC = 5.2 – 12.3%) and should be accounted for.

3. *Exposure-age calculation* – Recalibrated mean R-values and the mean absolute deviation for each sample are calculated and are used to generate Schmidt Hammer exposure ages and 1σ uncertainties for each sampled surface using the updated granite calibration curve presented in this paper (Fig. 5).

User inputs include sample IDs and locations (latitude/longitude), which are stored in a database for monitoring of site usage. User data (R-values and SH exposure ages) are not recorded. The analysis codes are compiled in Python and are available for users to access. With the exception of age calibration using the University of Manchester calibration boulder, users can sample deposits, perform instrument calibration and generate exposure ages and uncertainties independently. SHED-Earth further streamlines this dating technique by providing a rapid and accessible means of exposure age calculation. It is anticipated that as new regional calibration curves are generated in similar well-dated regions, they will be made available on SHED-Earth. Finally, for researchers developing their own regional TCN to R-value calibration curves, we are happy to host your data and make your curve an available option for other users.

Conclusions

Despite extensive research over the last ~40 years (c.f. Table 1; Tomkins *et al.*, 2016), previous studies have failed to inspire the Quaternary community at large to take up the Schmidt Hammer and integrate these data with newer dating methods. The recommendations in Dortch *et al.*, (2016) were intended to encourage Quaternary researchers to test and utilise our calibration curve and generate their own curves in suitably dated regions. Winkler and Matthews (2016) criticize Tomkins *et al.*, (2016) and Dortch *et al.*, (2016) for instrument and age calibration but fail to address the significantly larger uncertainties associated with age-calibration curve construction. Our calibration procedures produce realistic uncertainties, incorporate operator variance and are more effective on surfaces typically tested by Quaternary researchers, making them more appropriate than previous calibration procedures which are not specifically designed for the Quaternary community or for SHED. While we acknowledge that robust Schmidt Hammer calibration procedures are necessary to generate reliable data (McCarroll, 1987; McCarroll, 1994), it is evident that of greater concern in the application of SHED is the use of isolated age control points. The largest uncertainties are a consequence of limited data points for age-calibration curve construction, which is exacerbated by geological uncertainty associated with TCN exposure ages (Heyman *et al.*, 2011). To accommodate this uncertainty, calibration curves should be based on statistically large datasets to minimise individual exposure age uncertainty (c.f. Tomkins *et al.*, 2016). Our methods take a conservative view, incorporate larger uncertainties and still produced a robust age calibration curve for granite surfaces in the UK.

We hope that clear instrument and age calibration procedures, new exposure age data ($n = 29$) and the availability of an online-calculator which streamlines calibration and SHED exposure age calculation (<http://shed.earth>), will provide further encouragement for Quaternary researchers. The calibration dataset is now substantial ($n = 54$) and is applicable over the timeframe of 0.8 – 23.8 ka.

346 While we acknowledge that further work is necessary to apply the technique more widely to
347 undated landforms (e.g. Barr *et al.*, 2017), we believe that the current calibration is fully usable and
348 encourage researchers to test and utilize it.

349

350 References

- 351 André, M. F. (2002). Rates of postglacial rock weathering on glacially scoured outcrops (Abisko–Riksgränsen area,
352 68°N). *Geografiska Annaler: Series A, Physical Geography*, 84(3-4), 139-150. <https://doi.org/10.1111/j.0435-3676.2002.00168.x>
- 354 Aydin, A. (2009). The ISRM Suggested Methods for Rock Characterization, Testing and Monitoring: 2007-2014. *Int. J. Rock Mech. Min. Sci.*, 46, 627–634. <https://doi.org/10.1007/978-3-319-07713-0>
- 356 Ballantyne, C. K., McCarroll, D., & Stone, J. O. (2007). The Donegal ice dome, northwest Ireland: dimensions and
357 chronology. *Journal of Quaternary Science*, 22, 773–783. <https://doi.org/10.1002/jqs>
- 358 Ballantyne, C. K., & Stone, J. O. (2015). Trimlines, blockfields and the vertical extent of the last ice sheet in southern
359 Ireland. *Boreas*, 44, 277–287. <https://doi.org/10.1111/bor.12109>
- 360 Barr, I. D., Roberson, S., Flood, R., & Dortch, J. (2017). Younger Dryas glaciers and climate in the Mourne Mountains,
361 Northern Ireland. *Journal of Quaternary Science*, 32(1), 104–115. <https://doi.org/10.1002/jqs.2927>
- 362 Borchers, B., Marrero, S., Balco, G., Caffee, M., Goehring, B., Lifton, N., Nishiizumi, K., Phillips, F., Schaefer, J., & Stone, J.
363 (2016). Geological calibration of spallation production rates in the CRONUS-Earth project. *Quaternary Geochronology*,
364 31, 188-198. <https://doi.org/10.1016/j.quageo.2015.01.009>
- 365 Clark, J., Cabe, A. M. M. C., Schnabel, C., Clark, P. U., Freeman, S., Maden, C., & Xu, S. (2009). ¹⁰Be chronology of the last
366 deglaciation of County Donegal, northwestern Ireland. *Boreas*, 38, 111–118. <https://doi.org/10.1111/j.1502-3885.2008.00040.x>
- 368 Clark, J., McCabe, A. M., Bowen, D. Q., & Clark, P. U. (2012). Response of the Irish Ice Sheet to abrupt climate change
369 during the last deglaciation. *Quaternary Science Reviews*, 35, 100–115. <https://doi.org/10.1016/j.quascirev.2012.01.001>
- 370 Demirdag, S., Yavuz, H., & Altindag, R. (2009). The effect of sample size on Schmidt rebound hardness value of rocks.
371 *International Journal of Rock Mechanics and Mining Sciences*, 46(4), 725–730.
372 <https://doi.org/10.1016/j.ijrmms.2008.09.004>
- 373 Dortch, J. M., Hughes, P. D., & Tomkins, M. D. (2016). Schmidt hammer exposure dating (SHED): Calibration boulder of
374 Tomkins *et al.* (2016). *Quaternary Geochronology*, 35, 67–68. <https://doi.org/10.1016/j.quageo.2016.06.001>
- 375 Everest, J., & Kubik, P. (2006). The deglaciation of eastern Scotland: Cosmogenic ¹⁰Be evidence for a Lateglacial stillstand.
376 *Journal of Quaternary Science*, 21(1), 95–104. <https://doi.org/10.1002/jqs.961>
- 377 Finlayson, A., Fabel, D., Bradwell, T., & Sugden, D. (2014). Growth and decay of a marine terminating sector of the last
378 British–Irish Ice Sheet: a geomorphological reconstruction. *Quaternary Science Reviews*, 83, 28–45.
379 <https://doi.org/10.1016/j.quascirev.2013.10.009>
- 380 Golledge, N., Fabel, D., Everest, J. D., Freeman, S., & Binnie, S. (2007). First cosmogenic ¹⁰Be age constraint on the timing
381 of Younger Dryas glaciation and ice cap thickness, western Scottish Highlands. *Journal of Quaternary Science*, 22(8),
382 785–791. <https://doi.org/10.1002/jqs>
- 383 Goudie, A. S. (2006). Progress in Physical Geography The Schmidt Hammer in geomorphological research. *Progress in Physical Geography*, 30, 703–718. <https://doi.org/10.1177/0309133306071954>
- 385 Gunnell, Y., Jarman, D., Braucher, R., Calvet, M., Delmas, M., Leanni, L., Bourlès, D., Aumaître, G., & Keddaouche, K.
386 (2013). The granite tors of Dartmoor, Southwest England: Rapid and recent emergence revealed by Late Pleistocene
387 cosmogenic apparent exposure ages. *Quaternary Science Reviews*, 61, 62–76.
388 <https://doi.org/10.1016/j.quascirev.2012.11.005>
- 389 Heyman, J., Stroeven, A. P., Harbor, J. M., & Caffee, M. W. (2011). Too young or too old: Evaluating cosmogenic exposure
390 dating based on an analysis of compiled boulder exposure ages. *Earth and Planetary Science Letters*, 302(1–2), 71–80.
391 <https://doi.org/10.1016/j.epsl.2010.11.040>

- 392 Kirkbride, M., Everest, J., Benn, D., Gheorghiu, D., & Dawson, A. (2014). Late-Holocene and Younger Dryas glaciers in the
393 northern Cairngorm Mountains, Scotland. *The Holocene*, 24(2), 141–148. <https://doi.org/10.1177/0959683613516171>
- 394 Lal, D. (1991). Cosmic ray labeling of erosion surfaces: in situ nuclide production rates and erosion models. *Earth and*
395 *Planetary Science Letters*, 104(2-4), 424-439. [https://doi.org/10.1016/0012-821X\(91\)90220-C](https://doi.org/10.1016/0012-821X(91)90220-C)
- 396 Matthews, J. A., & Owen, G. (2008). Endolithic lichens, rapid biological weathering and Schmidt Hammer R-values on
397 recently exposed rock surfaces: Storbreen glacier foreland, Jotunheimen, Norway. *Geografiska Annaler, Series A:*
398 *Physical Geography*, 90(4), 287–297. <https://doi.org/10.1111/j.1468-0459.2008.00346.x>
- 399 Matthews, J. A., & Winkler, S. (2011). Schmidt-hammer exposure-age dating (SHD): Application to early Holocene
400 moraines and a reappraisal of the reliability of terrestrial cosmogenic-nuclide dating (TCND) at Austanbotnbreen,
401 Jotunheimen, Norway. *Boreas*, 40(2), 256–270. <https://doi.org/10.1111/j.1502-3885.2010.00178.x>
- 402 McCabe, A. M., Clark, P. U., & Clark, J. (2007). Radiocarbon constraints on the history of the western Irish ice sheet prior
403 to the Last Glacial Maximum. *Geology*, 35, 147–150. <https://doi.org/10.1130/G23167A.1>
- 404 Mccabe, A. M., & Williams, G. D. (2012). Timing of the East Antrim Coastal Readvance: phase relationships between
405 lowland Irish and upland Scottish ice sheets during the Last Glacial Termination. *Quaternary Science Reviews*, 58, 18–
406 29. <https://doi.org/10.1016/j.quascirev.2012.10.012>
- 407 McCarroll, D. (1987). The Schmidt hammer in geomorphology: five sources of instrument error. *Br. Geomorphol. Res. Group*
408 *Tech. Bull.*, 36, 16–27.
- 409 McCarroll, D. (1994). The Schmidt Hammer as a measure of degree of rock surface weathering and terrain age. In C. Beck
410 (Ed.), *Dating in Exposed and Surface Contexts* (pp. 29–45). Albuquerque: University of New Mexico Press.
- 411 Niedzielski, T., Migon, P., & Placek, A. (2009). A minimum sample size required from Schmidt hammer measurements. *Earth*
412 *Surface Processes and Landforms*, 34, 1713–1725. <https://doi.org/10.1002/esp>
- 413 Phillips, W. M., Hall, A. M., Ballantyne, C. K., Binnie, S., Kubik, P. W., & Freeman, S. (2008). Extent of the last ice sheet in
414 northern Scotland tested with cosmogenic ¹⁰Be exposure ages. *Journal of Quaternary Science*, 23(2), 101-107.
415 <https://doi.org/10.1002/jqs.1161>
- 416 Proceq. (2004). *Operating Instructions Betonprüfhammer N/NR- L/LR*. Schwerzenbach.
- 417 Riebe, C. S., Kirchner, J. W., & Finkel, R. C. (2004). Erosional and climatic effects on long-term chemical weathering rates in
418 granitic landscapes spanning diverse climate regimes. *Earth and Planetary Science Letters*, 224(3), 547-562.
419 <https://doi.org/10.1016/j.epsl.2004.05.019>
- 420 Small, D., Fabel, D. (2015). A Lateglacial ¹⁰Be production rate from glacial lake shorelines in Scotland. *Journal of Quaternary*
421 *Science*, 30, 509–513. <https://doi.org/10.1002/jqs.2804>
- 422 Small, D., & Fabel, D. (2016). Was Scotland deglaciated during the Younger Dryas? *Quaternary Science Reviews*, 145, 259–
423 263. <https://doi.org/10.1016/j.quascirev.2016.05.031>
- 424 Small, D., Rinterknecht, V., Austin, W., Fabel, D., Miguens-Rodriguez, M., & Xu, S. (2012). In situ cosmogenic exposure ages
425 from the Isle of Skye, northwest Scotland: Implications for the timing of deglaciation and readvance from 15 to 11ka.
426 *Journal of Quaternary Science*, 27(2), 150–158. <https://doi.org/10.1002/jqs.1522>
- 427 Stone, J. O. (2000). Air pressure and cosmogenic isotope production. *Journal of Geophysical Research: Solid Earth*,
428 105(B10), 23753-23759. <https://doi.org/10.1029/2000JB900181>
- 429 Sumner, P., & Nel, W. (2002). The effect of rock moisture on Schmidt hammer rebound: Tests on rock samples from
430 Marion Island and South Africa. *Earth Surface Processes and Landforms*, 27(10), 1137–1142.
431 <https://doi.org/10.1002/esp.402>
- 432 Tomkins, M. D., Dortch, J. M., & Hughes, P. D. (2016). Schmidt Hammer exposure dating (SHED): Establishment and
433 implications for the retreat of the last British Ice Sheet. *Quaternary Geochronology*, 33, 46–60.
434 <https://doi.org/10.1016/j.quageo.2016.02.002>
- 435 Viles, H., Goudie, A., Grab, S., & Lalley, J. (2011). The use of the Schmidt Hammer and Equotip for rock hardness
436 assessment in geomorphology and heritage science: A comparative analysis. *Earth Surface Processes and Landforms*,
437 36(3), 320–333. <https://doi.org/10.1002/esp.2040>
- 438 Von Blanckenburg, F., Bouchez, J., Ibarra, D. E., & Maher, K. (2015). Stable runoff and weathering fluxes into the oceans
439 over Quaternary climate cycles. *Nature Geoscience*, 8(7), 538. <https://doi.org/10.1038/ngeo2452>

- 440 Williams, R. B. G., & Robinson, D. A. (1983). The effect of surface texture on the determination of the surface hardness of
441 rock using the schmidt hammer. *Earth Surface Processes and Landforms*, 8(3), 289–292.
442 <https://doi.org/10.1002/esp.3290080311>
- 443 Wilson, K. R. (2004). The last glaciation in the Western Mourne Mountains, Northern Ireland. *Scottish Geographical Journal*,
444 120, 199–210. <https://doi.org/10.1080/00369220418737203>
- 445 Wilson, P., Lord, T., & Rodés, Á. (2013). Deglaciation of the eastern Cumbria glaciokarst, northwest England, as
446 determined by cosmogenic nuclide (^{10}Be) surface exposure dating, and the pattern and significance of subsequent
447 environmental changes. *Cave and Karst Science*, 40(1), 22–27.
- 448 Winkler, S. (2009). First attempt to combine terrestrial cosmogenic nuclide (^{10}Be) and Schmidt hammer relative-age dating:
449 Strauchon Glacier, Southern Alps, New Zealand. *Central European Journal of Geosciences*, 1(3), 274–290.
450 <https://doi.org/10.2478/v10085-009-0026-3>
- 451 Winkler, S., & Matthews, J. A. (2014). Comparison of electronic and mechanical Schmidt hammers in the context of
452 exposure-age dating: Are Q- and R-values interconvertible? *Earth Surface Processes and Landforms*, 39(8), 1128–1136.
453 <https://doi.org/10.1002/esp.3584>
- 454 Winkler, S., & Matthews, J. A. (2016). Inappropriate instrument calibration for Schmidt-hammer exposure-age dating (SHD)
455 – A comment on Dortch *et al.*, *Quaternary Geochronology* 35 (2016), 67–68. *Quaternary Geochronology*, 36, 102–
456 103. <https://doi.org/10.1016/j.quageo.2016.08.009>

457

459 **Acknowledgements**

460 We would like to thank C. Ballantyne, J. Clark, J. Everest and D. Small for providing sample
461 photographs which were essential when conducting fieldwork. D. Fabel also kindly provided
462 unpublished calibration data for the LLPR which permitted exposure age recalibration. We would
463 also like to thank R. Pope, T. Tonkin and D. Tomkins for fieldwork assistance and J. Nudds for
464 advice on suitable surfaces to sample. This study was partially funded by the University of
465 Manchester SEED Fieldwork Support Fund. Hughes and Dortch would like to thank the University of
466 Manchester Research Stimulation Fund.

Figure Captions

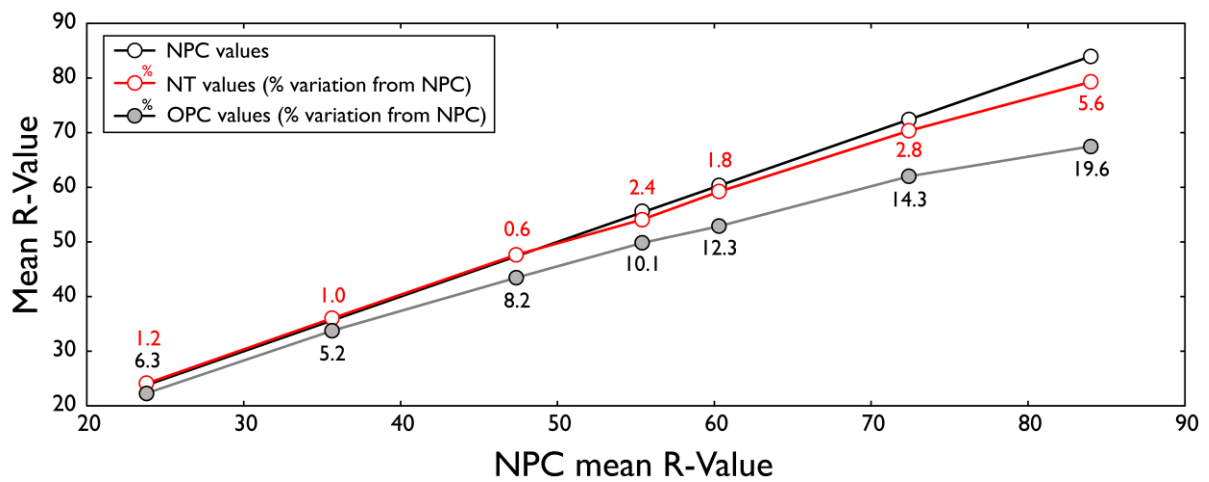


Fig. 1. Uncalibrated mean R-values for tested surfaces using the NPC, OPC and NT Schmidt Hammers.

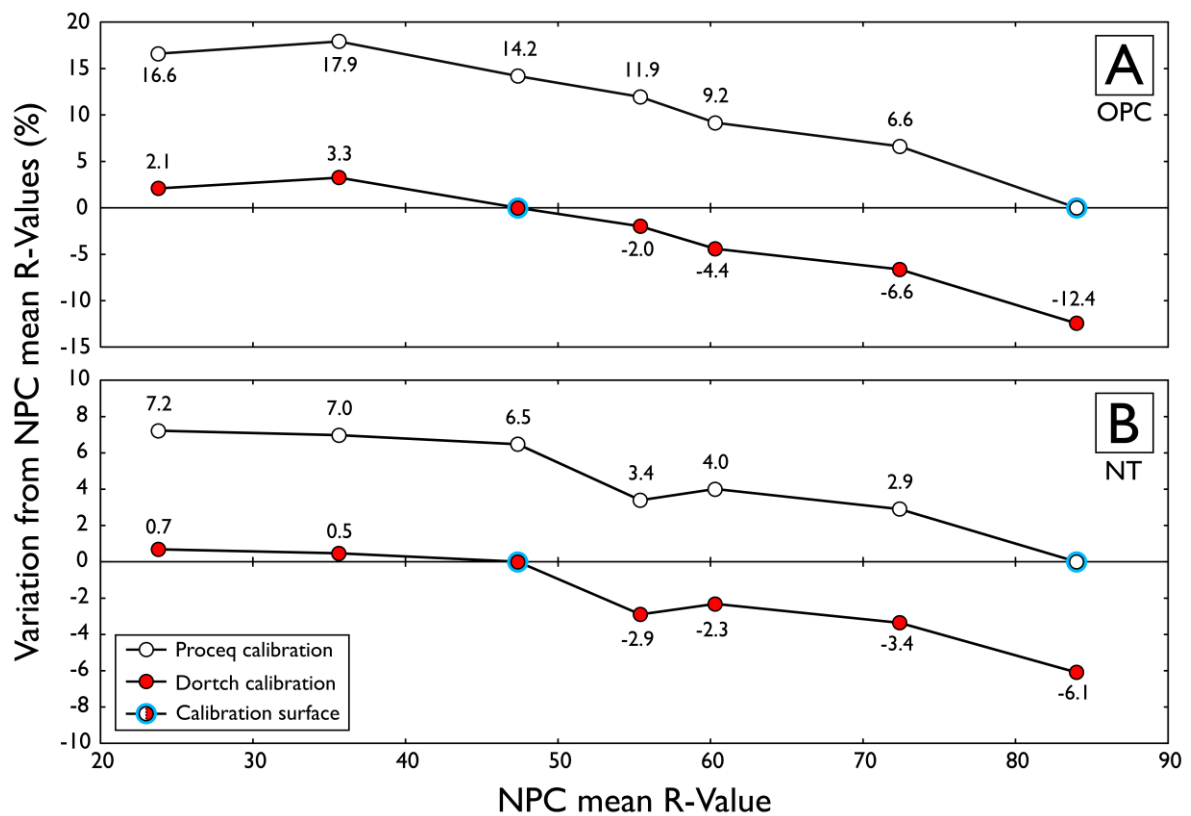


Fig. 2. Recalibrated mean R-values for tested surfaces using Proceq (2004) and Dortch et al. (2016) calibration procedures for the (A) OPC and (B) NT Schmidt Hammers.

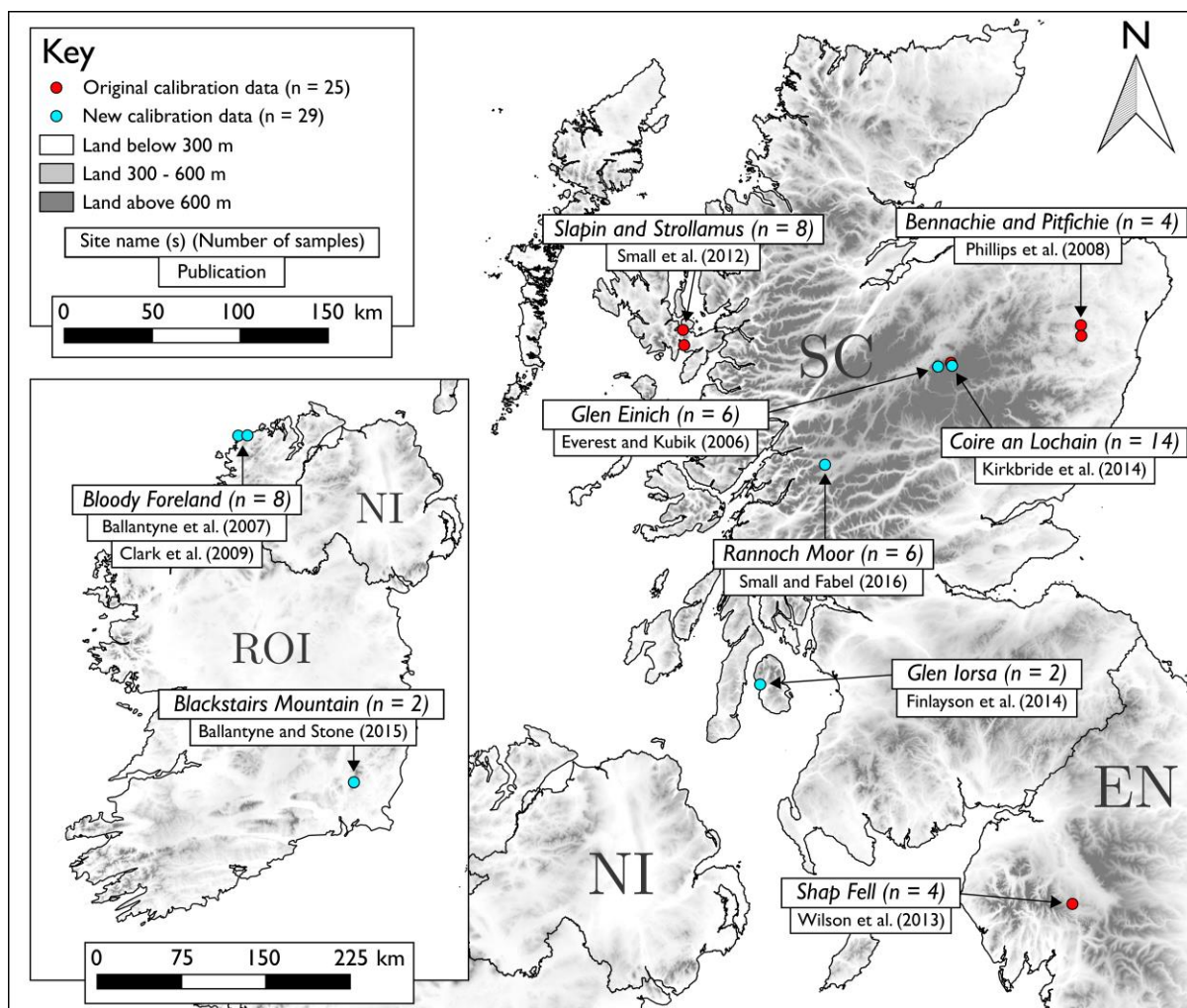


Fig. 3. Sample map showing the location of original (n = 25) and new calibration surfaces (n = 29) from across Scotland and NW England, including new sampled surfaces from Coire an Lochain (Kirkbride *et al.*, 2014), Rannoch Moor (Small and Fabel, 2016), Glen Einich (Everest and Kubik, 2006) and Glen Iorsa (Finlayson *et al.*, 2014). New early (> 20 ka) post-LGM samples from Ireland on Blackstairs Mountain, Wexford (Ballantyne and Stone, 2015) and at Bloody Foreland, Donegal (Ballantyne *et al.*, 2007; Clark *et al.*, 2009) are shown inset.

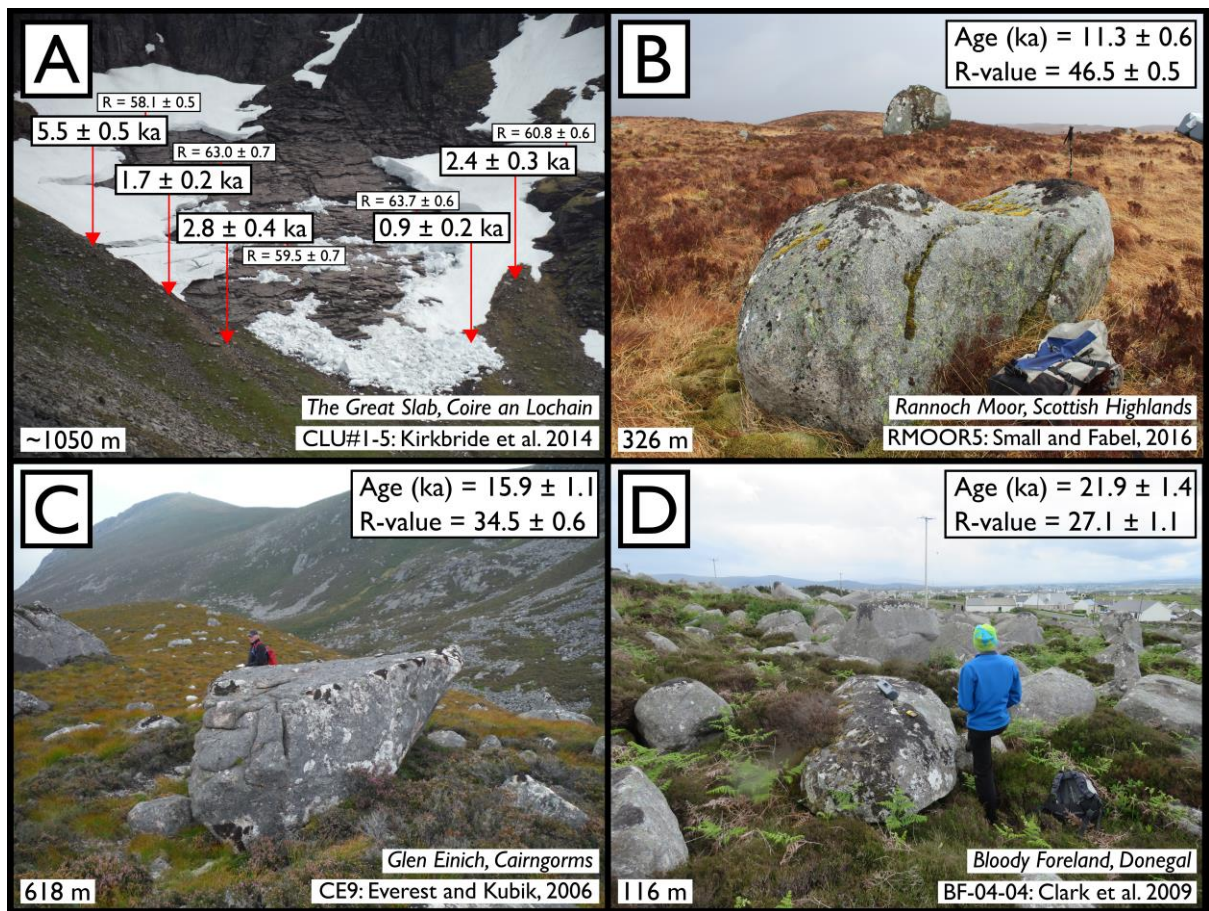


Fig. 4. Sample photos for (A) Holocene, (B) Younger Dryas, (C) Lateglacial Interstadial and (D) early post-LGM samples, displaying LLPR exposure ages (Fabel *et al.*, 2012), calibrated mean R-values, and sample elevations. The spread of exposure ages in Coire an Lochain (A) likely reflects the variable exposure of cliff surfaces to cosmogenic radiation (Kirkbride *et al.*, 2014).

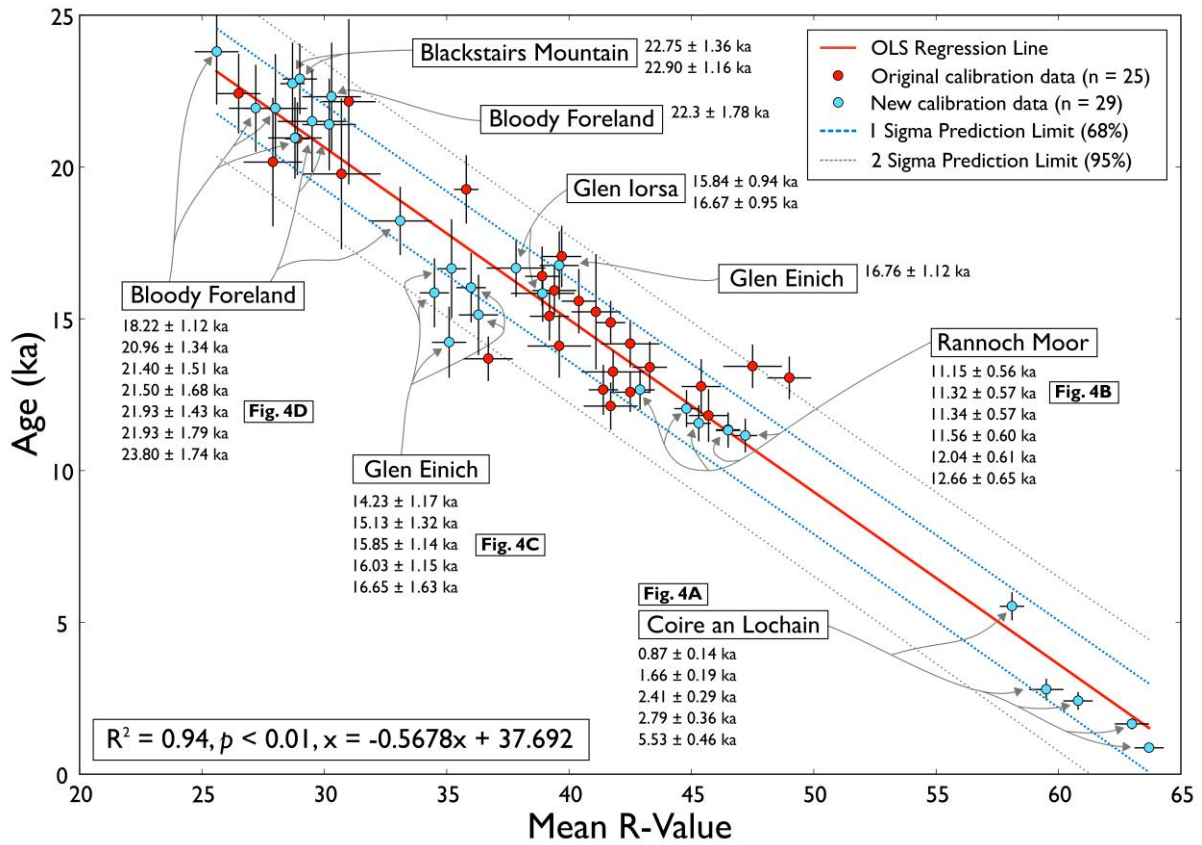


Fig. 5. Updated regional calibration curve for the British Isles (n = 54), displaying the least squares regression line (red), 1σ (blue) and 2σ (grey) prediction limits, and sample exposure ages for each new calibration site.

Table Captions

Table I. Information on tested surfaces, raw R-value data for the NPC, NT and OPC Schmidt Hammers and T-test results.

Tested Surface	Location ^a	Latitude (°)	Longitude (°)	Mean R Values ^b						Difference from NPC (%)		T-test Results ^c		T-test Interpretations ^d	
				NPC	±	NT	±	OPC	±	NT	OPC	NT	OPC	NT	OPC
Test anvil	Arthur Lewis Building (interior)	-	-	84.0	0.0	79.3	0.7	67.5	2.6	5.6	19.6	< 0.01	< 0.01	H ₁	H ₁
Borrowdale Volcanic Group erratic	Old Quadrangle	53.465740	-2.234289	72.4	2.4	70.4	2.7	62.0	1.5	2.8	14.3	0.02	< 0.01	H ₁	H ₁
Polished Sandstone boulder	Bridgeford Street (rock garden)	53.466687	-2.235000	60.3	1.5	59.2	2.7	52.9	1.7	1.8	12.3	0.14	< 0.01	H ₀	H ₁
Marble pillar	Arthur Lewis Building (exterior)	53.466589	-2.235202	55.4	1.3	54.1	1.2	49.8	0.7	2.3	10.0	< 0.01	< 0.01	H ₁	H ₁
Doddington Sandstone boulder	Bridgeford Street (rock garden)	53.466639	-2.234881	47.4	1.9	47.6	2.1	43.5	1.8	-0.6	8.2	0.67	< 0.01	H ₀	H ₁
Concrete block	Bridgeford Street	53.466516	-2.234713	35.6	2.5	36.0	1.8	33.8	2.5	-1.0	5.2	0.61	0.02	H ₀	H ₁
Breezeblock	Arthur Lewis Building (interior)	-	-	23.8	1.4	24.1	1.7	22.3	1.2	-1.3	6.3	0.59	< 0.01	H ₀	H ₁

^a University of Manchester properties, ^b Uncertainty estimates (±) are the mean absolute deviation, ^c p-values of two sample Student t-tests assuming unequal variance, ^d H₁ = the difference between the two population means is statistically significant, H₀ = the difference between the two population means is not statistically significant

Table 2. Calibration results using the Proceq (2004) and Dortch et al. (2016) calibration procedures for the OPC and NT Schmidt Hammers and comparison with baseline NPC R-values.

Proceq calibration ^a		Dortch calibration ^a		Proceq variance (%) ^f		Dortch variance (%) ^f		Preferred calibration method ^g
NT ^b	OPC ^c	NT ^d	OPC ^e	NT	OPC	NT	OPC	
84.0	84.0	78.9	73.6	0.0	0.0	-6.1	-12.4	<i>Proceq</i>
74.5	77.2	70.0	67.6	2.9	6.6	-3.4	-6.6	<i>Proceq</i>
62.7	65.8	58.9	57.6	4.0	9.2	-2.3	-4.4	<i>Dortch</i>
57.3	62.0	53.8	54.3	3.4	11.9	-2.9	-2.0	<i>Dortch</i>
50.4	54.1	47.4	47.4	6.5	14.2	0.0	0.0	<i>Dortch</i>
38.1	42.0	35.8	36.8	7.0	17.9	0.5	3.3	<i>Dortch</i>
25.5	27.8	24.0	24.3	7.2	16.6	0.7	2.1	<i>Dortch</i>

^a Using correction factors of ^b1.05882: ^c1.24444, ^d0.994: ^e1.08972, ^f with respect to mean NPC R-values, ^g based on minimising the % variation between recalibrated R-values and the NPC